Association Model for Nickel and Vanadium with Asphaltene during Solvent Deasphalting

ARTICLE *in* ENERGY & FUELS · MARCH 2015

Impact Factor: 2.79 · DOI: 10.1021/ef502696p

7 AUTHORS, INCLUDING:

Linzhou Zhang

China University of Petroleum

16 PUBLICATIONS **47** CITATIONS

SEE PROFILE

Xuewen Sun

China University of Petroleum

299 PUBLICATIONS **6,435** CITATIONS

SEE PROFILE

Chunming Xu

China University of Petroleum

213 PUBLICATIONS **2,642** CITATIONS

SEE PROFILE

Suoqi Zhao

China University of Petroleum

95 PUBLICATIONS **1,077** CITATIONS

SEE PROFILE

energy&fuels

Article

pubs.acs.org/EF

Association Model for Nickel and Vanadium with Asphaltene during Solvent Deasphalting

Chuanbo Yu, Linzhou Zhang, Xiuying Guo, Zhiming Xu, Xuewen Sun, Chunming Xu, and Suoqi Zhao*

State Key Laboratory of Heavy Oil Processing, China University of Petroleum, Beijing 102249, People's Republic of China

ABSTRACT: Solvent deasphalting is a highly efficient process for removing asphaltene and metals from the petroleum residue; however, there are rare modeling studies about the interaction between metals and asphaltene. This work establishes the association models of metals (Ni and V) with asphaltene during solvent deasphalting. The models reveal that the distribution factors of metals are related to the solvent density, association enthalpy, and temperature. The association energy of metal−asphaltene is higher than that of metal−resin. The distribution factor of metals with asphaltene is lower than that without asphaltene. The tuned model could well-predict the distribution factors for both Ni and V. The models provide the thermodynamics and theoretical guide for removing the metals from the heavy oil during solvent deasphalting.

1. INTRODUCTION

Highly efficient utilization of residue oils is very important for the petroleum-refining industry. Two main conversion approaches are the carbon-rejecting and hydrogen-adding approaches. However, the high content of metals and asphaltene leads to the conventional conversion approaches becoming very difficult, costly, or even not applicable.[1,2]

The crude oil electrical desalting process can remove most metals, such as Na, Ca, and Mg, but Ni and V are very difficult to be removed, which are mostly present in the forms of vanadyl porphyrins and nickel porphyrins. These petroporphyrins are concentrated in the high-boiling-point residua and often composed of or associated with heavy oil molecules (preferentially for asphaltene or resin). For convenience, the "metal" only relates to "Ni" and "V" in this work.

The solvent deasphalting process (SDA) uses the light paraffin as a solvent to extract residue to obtain a deasphlated oil (DAO) and a de-oiled asphaltene (DOA). The primary purpose is removing asphaltene and metals from petroleum residue.[3−6] The SDA process is highly efficient for demetalization, although the mechanism is not well explained. The reason is the poor knowledge on the metal compound structure and its interaction with asphaltene.

Miller et al.[7] determined the local structure of non-porphyrin Ni and V in the Maya residue, hydrocracked residue, and toluene-insoluble solid using X-ray absorption fine structure (XAFS) spectroscopy. XAFS revealed that (i) the porphyrin structure and the non-porphyrin structure of Ni and V display different ultraviolet−visible (UV−vis) spectra, (ii) the local structure, coordination geometry, and bond distances of three raw materials are similar, and (iii) the association structure of three materials is similar in high stability. Rodgers et al.[8] identified the metals [Ni(II) or V═O(II)] and porphyrin type [e.g., etio versus deocophylerythro-etioporphyrin (DPEP)] by isolation and subsequent Fourier transform ion cyclotron resonance electrospray ionization mass spectrometry (FT-ICR−ESI MS). McKenna et al.[9] identified vanadyl porphyrins by atmospheric pressure photoionization (APPI) FT-ICR MS. A total of 12 types of vanadyl porphyrins had been identified in a raw Athabasca bitumen asphaltene fraction, and a total of 7 types of double bond equivalent (DBE) distribution of vanadyl porphyrin had been identified in the South American heavy oil. Qian et al.[10] identified nickel porphyrins by APPI FT-ICR MS. Porphyrins containing sufur[11] and oxygen[12] heteroatoms had also been identified. Shiraishi et al.[13] developed the demetalation process for residue oils based on a combination of the photochemical reaction and liquid−liquid extraction. This process was easy to demetalize "free type" metalloporphyrins but difficult to demetalize "bond type" metalloporphyrins. Gray et al.[14] separated the petroporphyrins from asphaltenes using the chemical modification and selective affinity chromatography. The limitations of the approach likely result from the aggregation of asphaltene with a vanadium component. Chen et al.[15] studied the model of vanadium porphyrin adsorption to C_7-asphaltene in pentane solution. The molecular evidence of adsorption was identified using transmission electron microscopy (TEM), FT-ICR MS, and Brunauer−Emmett−Teller (BET). The thermodynamic calculation showed that strong interaction exists between porphyrin and asphaltene.

The above works showed that (i) Ni and V species are various porphyrins, (ii) the separation of metal porphyrins from asphaltene is quite difficult, and (iii) the separation of metal porphyrins associated with asphaltene from a petroleum residue might be a practical way, instead of separating porphyrin from asphaltene.[15] However, there are rare modeling studies about the interaction between metal and asphaltene; moreover, there are some difficulties in modeling the interaction because heavy oils are complicated mixtures.

For the complicated mixture, the Chrastil association model[16] could often provide a good correlation for the solubility of solute of solid or liquid during the supercritical fluid extraction. Moreover, because the model has only three parameters and high precision, it has widely been used to model the solubility in sub- and supercritical fluids.[17] Zhao et al.[18] correlated the

Received: December 2, 2014
Revised: February 11, 2015
Published: February 12, 2015

DOI: 10.1021/ef502696p
Energy Fuels 2015, 29, 1534−1542

extraction yield of heavy oil in supercritical pentane and isobutane. Eslamimanesh et al.[19,20] determined the sulfur and glycol contents of in supercritical gases. Galán et al.[21,22] studied solubility of kerogen from oil shales in supercritical toluene and methanol. Gutiérrez et al.[23] performed a theoretical design about the separation column of essential oils in supercritical carbon dioxide.

Synthesized the extraction and fractionation of heavy oil,[24,25] selective solvent deasphalting,[26] characterization of heavy oil,[27−29] Chrastil association theory,[16] and adsorption evidence between porphyrin and asphaltene,[15] we try to establish the semi-empirical association model between metals and asphaltene. This work investigates and discusses four aspects: (i) the Ni and V contents and their distributions during the SDA process, (ii) the theoretical analysis and experimental validation of the association model between metals and asphaltene, (iii) the physical significance of model parameters, and (iv) the prospect of model application during the SDA process.

2. EXPERIMENTAL SECTION

2.1. Supercritical Fluid Extraction and Fractionation (SFEF). In the past, we established a stage SFEF, which has successfully been used for detailed characterization of over 50 kinds of petroleum residua. Typical schematics for SFEF separation equipment have been published elsewhere.[24,25] To ensure the separation under equilibrium, SFEF used a synthetical operation: (i) the solvent state is controlled in the range of sub- and supercritical by adjusting the temperature and pressure; (ii) the temperature gradient of the separation column is fixed, (iii) the pressure rises slowly; and (iv) the solvent circulation rate is changed from high to low. The criterion of equilibrium is until the yields of each fraction and their various properties [molecular weight (MW), density, saturates, aromatics, resins, and asphaltenes (SARA) components, etc.] are changeless. For 1000 g of residua, the yield of the extraction fraction is 1.4 g/min. Per 50 g is collected as one cut. About 14 cuts could be collected from the conventional residua. The typical separation conditions are as follows: solvent, pentane; temperature gradient from bottom to top, from 220 to 230 to 240 °C; pressure range and change rate, 4.0−12.0 MPa in 8 h; flow rate of solvent, 100 mL/min; weight of feedstock, 800−1000 g; and weight of each cut, 50 g.

2.2. Selective Extraction and Deasphalting Process (SELEX-Asp). Recently, we investigated systematically the deep SELEX-Asp, which had successfully been applied into the pilot instrument with 10 kg/h capacity and demonstration plant with 500 barrels/day.[30] SELEX-Asp has three separation stages: (i) the first stage (named SDA-1) is used to obtain the DOA, where the oil plus resin was separated from asphalt; (ii) the second stage (named SDA-2) is used to obtain the DAO (oil plus resin); and (iii) the third stage is designed for recovering the solvent under a supercritical state. The separation conditions (temperature, pressure, solvent/feedstock ratio, and feedstock properties) have been optimized to ensure the equilibrium separation. The criterion of equilibrium is until the yields of DOA and DAO and their various properties (MW, density, SARA components, etc.) are changeless. The typical separation conditions as follows: solvent, pentane; temperature of the first stage, from 150 to 180 °C; temperature of the second stage, from 160 to 190 °C; pressure, 5.0 MPa; and ratio of solvent/oil, 4:1.

2.3. Analysis Methods. The analysis of SARA components was determined by ASTM D2007-11. The number-average molecular weight of oil samples was determined using a Knauer-7000 vapor pressure osmometer at 60 °C and using toluene as the solvent according to ASTM D2503-92(2012). The density of oil samples was determined by ASTM D2320-98(2012). Ni and V contents of oil samples were determined by Vista-PRO simultaneous inductively coupled plasma−optical emission spectroscopy (ICP−OES). The pretreatment of the sample is decomposed with acid according to test method B of ASTM D5708-12. The conventional mass of the oil sample is 10−20 g, and the relative standard deviation (RSD) of the metal content is <5%. Light fractions 1−6 of SFEF are added up to 100 g for concentrating metals, and the RSD of the metal content is <10%.

2.4. Feedstock Properties. Two heavy petroleum residua were studied in this research. One is a 350 °C+ atmospheric residue of the *in situ* heavy oil (Orinoco, Venezuela), named AR. Another is a 500 °C+ vacuum residue of the Merry-16 blend extra heavy oil, named VR. The properties of the two residua are listed in Table 1. The two residua contain high contents of metals and asphaltene, which are favorable for studing the interaction of metals and asphaltene.

Table 1. Properties of Two Heavy Oil Residua

properties	AR 350 °C+	VR 500 °C+
density at 20 °C (g/cm^3)	1.0303	1.0343
API (deg)	5.8	5.3
CCR (wt %)	18.44	23.27
S (wt %)	4.4	3.7
N (wt %)	0.85	1.07
C (wt %)	84	84.39
H (wt %)	10.11	10.05
H/C	1.44	1.42
Ni (ppm)	126	134
V (ppm)	549	653
saturates (wt %)	20.01	17.28
aromatics (wt %)	40.41	39.71
resins (wt %)	26.76	27.79
C_7-asphaltenes (wt %)	12.13	13.68

3. THEORETICAL SECTION

3.1. Association Model of Metal Species in the SDA Process. *3.1.1. Association Model in the Rich-Solvent Extract Phase.* In petroleum or petroleum residue, the common assumption was that the metal species is associated with asphaltene or resin. In the extract phase of SDA, the DAO is generally associated with several solvent molecules. Evidently, there is a ternary system of metal species (Me), DAO (O), and solvent (S) in the SDA process. On the basis of the theoretical analysis (see the Appendix), here, we extend the Chrastil model from the binary system to this ternary system. It assumes that one ternary association molecule is composed of one metal molecule, one DAO molecule, and n molecules of solvent.

$$\mathrm{Me} + \mathrm{O} + n\mathrm{S} \rightleftarrows \mathrm{Me{\cdot}O{\cdot}S}_n \tag{1}$$

The solution equilibrium constant K_S can be expressed as follows in eq 2.

$$K_S = \frac{[\mathrm{Me{\cdot}O{\cdot}S}_n]}{[\mathrm{Me}][\mathrm{O}][\mathrm{S}]^n} \tag{2}$$

The temperature relation of K_S can be expressed by the Van't Hoff equation

$$\ln K_S = \frac{\Delta H_S}{RT} + q_S \tag{3}$$

where ΔH_S is the solvation enthalpy of metal−DAO−solvent in the SDA process and q_S is the constant.

3.1.2. Association Model in the Rich-Asphaltene Bottom Phase. Although in the extract phase of SDA, the metal association model is a ternary system of metal−DAO−solvent, for the bottom phase, the metal association model can be simplified as a binary system.

DOI: 10.1021/ef502696p
Energy Fuels 2015, 29, 1534−1542

In the bottom phase of the common deasphalting column (here, including SDA-1 and SFEF), the asphaltene is rich (>40%), where the asphaltene is the major association carrier for metals. However, in the bottom phase of the DAO column (here, corresponding to SDA-2), the asphaltene becomes very poor (0−5%) and the resin is rich (10−50%), where the resin is the major association carrier for metals. Furthermore, in the bottom phase of common SDA, the content of solvent is very low. It indicates that the solvation affection is slight and negligible.

Therefore, in the bottom phase of a common SDA process, the association of metals mainly depends upon the interaction between metal species and asphaltene. The association equilibrium is assumed as eq 4. The association equilibrium constant K_A can be expressed as eq 5. The temperature relation of K_A can be expressed by eq 6

$$\mathrm{Me} + \mathrm{Asp} \rightleftarrows \mathrm{Me{\cdot}Asp} \tag{4}$$

where Me, Asp, and Me·Asp represent metal species, asphaltene, and their associations

$$K_A = \frac{[\mathrm{Me{\cdot}Asp}]}{[\mathrm{Me}][\mathrm{Asp}]} \tag{5}$$

$$\ln K_A = \frac{\Delta H_A}{RT} + q_A \tag{6}$$

where ΔH_A is the association enthalpy of metal−asphaltene and q_A is the constant.

3.1.3. Association Model in the Poor-Asphaltene and Rich-Resin Bottom Phase. In the SDA-2, the association of metals mainly depends upon the interaction between metal species and resin. The association equilibrium was assumed as eq 7. The association equilibrium constant K_R can be expressed as eq 8. The temperature relation of K_R can be expressed by eq 9

$$\mathrm{Me} + \mathrm{Re} \rightleftarrows \mathrm{Me{\cdot}Re} \tag{7}$$

where Me, Re, and Me·Re represent metal species, resin, and their associations

$$K_R = \frac{[\mathrm{Me{\cdot}Re}]}{[\mathrm{Me}][\mathrm{Re}]} \tag{8}$$

$$\ln K_R = \frac{\Delta H_R}{RT} + q_R \tag{9}$$

where ΔH_R is the association enthalpy of metal−resin and q_R is the constant.

3.2. Distribution Factor of Metal Species in the SDA Process. *3.2.1. Definition of the Distribution Factor of Metal.* The distribution factor of metal species α_{Me} between the extraction phase and bottom phase can be expressed as

$$\alpha_{Me} = \frac{c_{Me,E}/c_{O,E}}{c_{Me,B}/c_{O,B}} \tag{10}$$

where α_{Me} is measured and calculated at a solvent-free basis, $c_{Me,E}$ is the metal content in extract oil in g/L, $c_{O,E}$ is the oil content in the extract phase in g/L, $c_{Me,B}$ is the metal content in the bottom residue in g/L, and $c_{O,B}$ is the total oil content in the bottom residue in g/L (including SARA components).

3.2.2. Distribution Factor of Metal between the Rich-Solvent and Rich-Asphaltene Phases. The detailed expression for the distribution factor of metal is derived in the Appendix

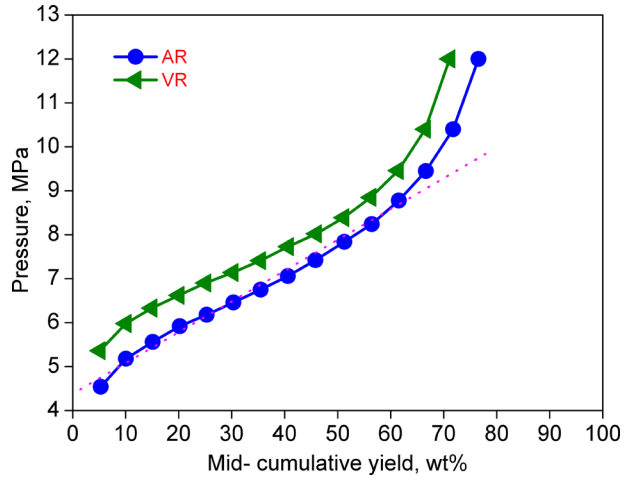

Figure 1. Extraction yields for SFEF cut under linear-increased pressure.

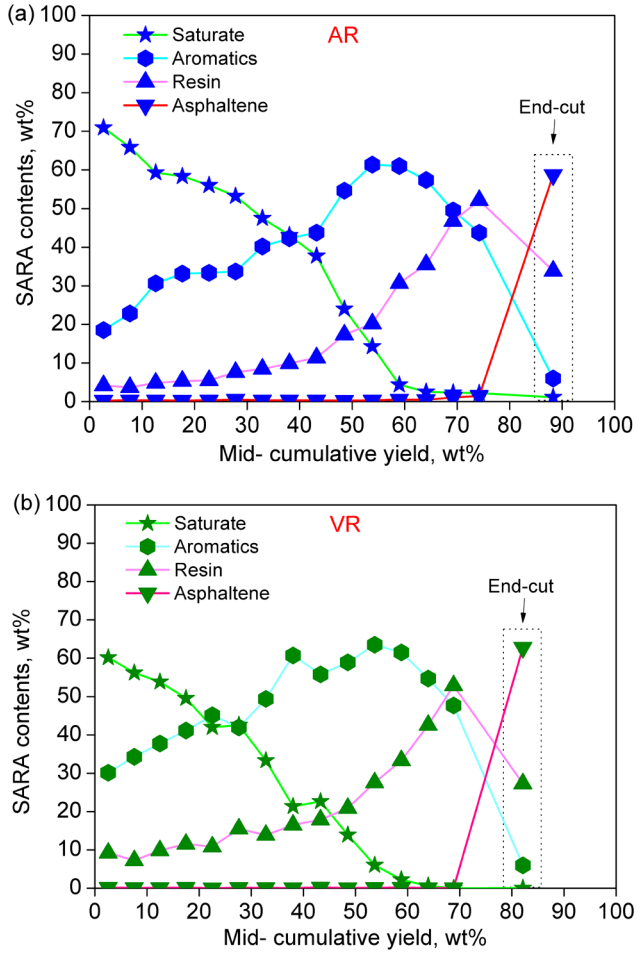

Figure 2. SARA contents for SFEF cut: (a) AR and (b) VR.

$$\ln \alpha_{Me} = n \ln \rho_S + \frac{\Delta H_1}{RT} + b_1 \tag{11}$$

$$\Delta H_1 = \Delta H_S - \Delta H_A \tag{12}$$

where n is the solvent association number, ρ_S is the solvent density in g/cm^3, ΔH_1 is the difference between the solvation enthalpy of metal−DAO−solvent and the association enthalpy of metal−asphaltene, and b_1 is assumed as a constant.

DOI: 10.1021/ef502696p
Energy Fuels 2015, 29, 1534−1542

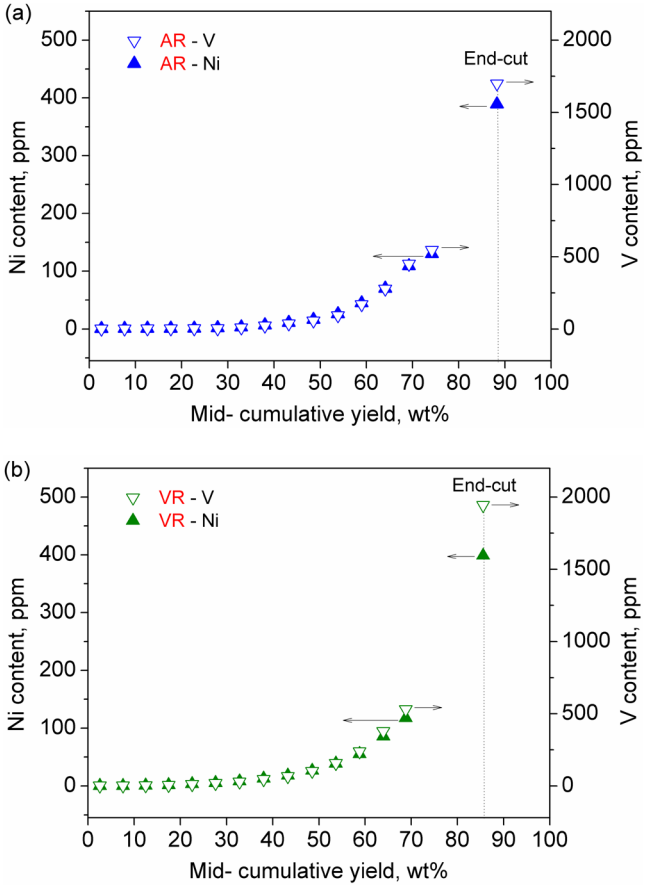

Figure 3. Ni and V contents for SFEF cut: (a) AR and (b) VR.

3.2.3. Distribution Factor of Metal between the Rich-Solvent and Rich-Resin Phases. The detailed expression for the distribution factor of metal is derived in the Appendix

$$\ln \alpha_{Me} = n \ln \rho_S + \frac{\Delta H_2}{RT} + b_2 \quad (13)$$

$$\Delta H_2 = \Delta H_S - \Delta H_R \quad (14)$$

where n is the solvent association number, ρ_S is the solvent density in g/cm^3, ΔH_2 is the difference between the solvation enthalpy of metal−DAO−solvent and the association enthalpy of metal−resin, and b_2 is assumed as a constant.

4. RESULTS AND DISCUSSION

4.1. SARA Distribution for SFEF. Figure 1 shows the SFEF yields for two residua. The mid-cumulative yield of cuts gradually increases with the pressure growth. AR is separated into 15 cuts and 1 unextractable end cut, and VR is separated into 14 cuts and 1 end cut.

Figure 2 shows the SARA compositions for SFEF cuts. The SARA trends are similar for two residua: (i) the contents of saturates decrease from 60−70% to nearly 0%; (ii) the aromatics rise from 20−30% to a maximum of 60−70% and then drop; (iii) the resins rise gradually from 10−20 to 50%; and (iv) the C_7-asphaltenes are generally below 0.5 wt %. However, in the end cut, C_7-asphaltenes of AR and VR rise to 58.7 and 52.9 wt %, respectively. Evidently, the asphaltenes are enriched in the unextractable end cut. The asphaltene amount in the bottom phase is almost unchanged in the SFEF process. Hence, the distribution of metals can be calculated on the basis of the balance between the extract phase and bottom phase.

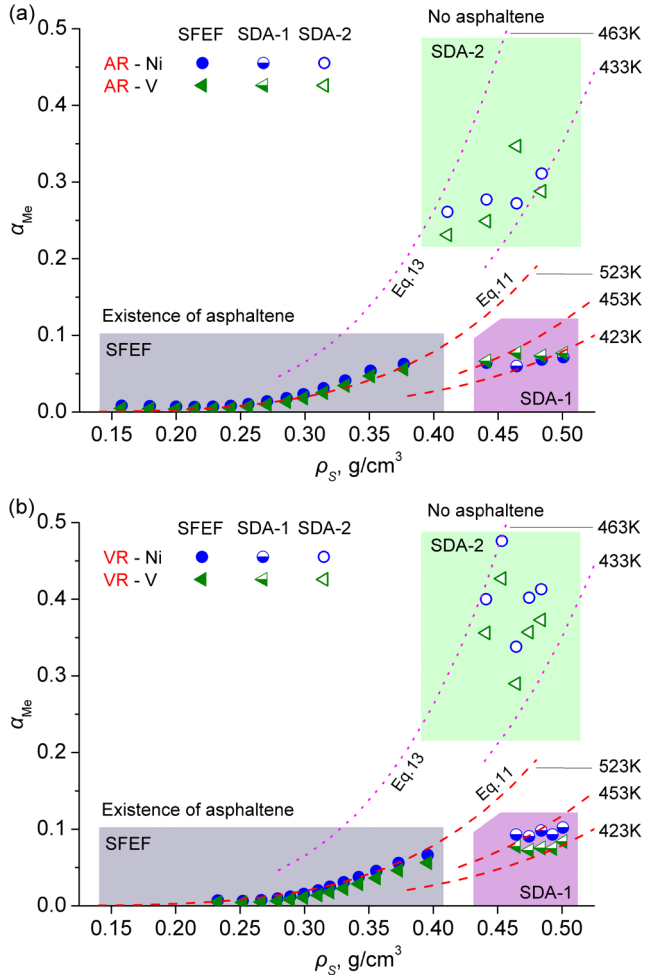

Figure 4. Ni and V distribution factors based on solvent free during pentane solvent deasphalting in SFEF (gray area), SDA-1 (purple area), and SDA-2 (green area): (a) AR and (b) VR.

4.2. Ni and V Contents for SFEF, SDA-1, and SDA-2. Figure 3 shows the Ni and V contents for SFEF cuts. The trends are similar for two residua: (i) Ni content rises gradually from 0.5 to 130 ppm, and (ii) V content rises gradually from 1.5 to 540 ppm. Correspondingly, Figure 2 shows that the resin content of cuts rises gradually from 10−20 to 50% and asphaltene is poor. However, in the end cut, Ni and V contents rise up to 380−400 and 1700−2000 ppm, respectively. Correspondingly, Figure 2 shows that the asphaltene content of the end cut is 52.9−58.7 wt %. In combination of Figures 2 and 3, higher Ni and V contents in petroleum are generally coupled by a higher asphaltene content.

Table 2 and 3 list the Ni and V contents of extract oil in SDA-1 and SDA-2, respectively. The results show that Ni and V contents in SDA-1 are much higher than those in SDA-2. Here, it is noted that the distribution factor in SDA-1 is lower than that in SDA-2, as discussed in a latter section.

4.3. Ni and V Distribution Factors for SFEF, SDA-1, and SDA-2. Although the Ni and V contents in SFEF and SDA-1 are higher than those in SDA-2, the distribution factors display an inverse trend. Figure 4 depicts the range of the distribution factor in SFEF (gray area), SDA-1 (purple area),

DOI: 10.1021/ef502696p
Energy Fuels 2015, 29, 1534−1542

Table 2. Ni and V Distributions in SDA-1 (5.0 MPa; S/O = 4:1, wt/wt)

	AR				VR				
temperature (K)	423	433	443	453	423	428	433	438	443
solvent density (g/cm^3)	0.5007	0.4839	0.4644	0.4410	0.5007	0.4926	0.4839	0.4745	0.4644
yield (wt %)	76.66	74.87	73.65	69.75	70.89	70.67	68.02	67.47	66.12
$c_{O,E}$ (g/L)	98.4	93.1	88.0	79.5	91.6	89.9	85.2	82.9	79.7
$c_{Ni,E}$ (ppm)	31.2	28.5	24.5	23.3	37.7	34.8	34.1	31.5	31.2
$c_{V,E}$ (ppm)	144	131	132	105	156.4	141.4	133	126.5	130.1
$c_{Ni,B}$ (ppm)	437	417	410	363	370	374	347	348	336
$c_{V,B}$ (ppm)	1880	1793	1715	1574	1862	1885	1758	1744	1673
α_{Ni} (experimental)	0.0714	0.0684	0.0598	0.0641	0.102	0.093	0.0982	0.0906	0.0930
α_{Ni} (calculated)	0.0690	0.0686	0.0659	0.0602	0.1019	0.0992	0.0957	0.0915	0.0865
α_{V} (experimental)	0.0766	0.0732	0.0770	0.0664	0.0840	0.0750	0.0756	0.0725	0.0778
α_{V} (calculated)	0.0792	0.0768	0.0714	0.0628	0.0820	0.0800	0.0774	0.0739	0.0698

Table 3. Ni and V Distributions in SDA-2 (5.0 MPa; S/O = 4:1, wt/wt)

	AR				VR				
temperature (K)	433	443	453	463	433	438	443	448	453
solvent density (g/cm^3)	0.4839	0.4644	0.441	0.4107	0.4839	0.4745	0.4644	0.4533	0.441
yield (wt %)	64.82	60.52	55.36	43.51	49.1	49.06	30.52	37.52	28.78
$c_{O,E}$ (g/L)	95.1	83.3	90	54.2	103.1	91.2	56.6	79.3	64.4
$c_{Ni,E}$ (ppm)	11.84	14.35	18.29	26.24	21.79	21.61	37.5	29.95	37.34
$c_{V,E}$ (ppm)	21.7	19	14.7	12.7	26.2	23.9	16.4	21.2	16.9
$c_{Ni,B}$ (ppm)	83.3	68.5	54.1	40.8	63.5	59.5	48.5	44.5	42.2
$c_{V,B}$ (ppm)	411	334	259	188	276.5	255.5	195.2	185.6	180.7
α_{Ni} (experimental)	0.311	0.272	0.277	0.261	0.413	0.402	0.338	0.476	0.400
α_{Ni} (calculated)	0.291	0.299	0.280	0.245	0.389	0.403	0.412	0.415	0.410
α_{V} (experimental)	0.288	0.347	0.249	0.231	0.373	0.357	0.290	0.427	0.356
α_{V} (calculated)	0.308	0.307	0.275	0.229	0.347	0.359	0.367	0.368	0.362

Table 4. Regressed Parameters for the Model

raw material	metal species	n	ΔH_1 (kJ/mol)	b_1	ΔH_2 (kJ/mol)	b_2	$\Delta H_A - \Delta H_R$ (kJ/mol)
AR	Ni	4.14	−20.7	6.068	−46.7	14.587	−26.0
	V	4.87	−20.5	6.663	−60.8	18.956	−40.3
VR	Ni	4.87	−15.7	5.573	−41.0	13.991	−25.3
	V	5.47	−19.5	6.843	−44.9	15.387	−25.4
average		4.82	−19.1	6.282	−48.4	15.730	−29.3

and SDA-2 (green area). The distribution factors for both SFEF and SDA-1 are much lower than those for SDA-2. The reason is that (i) in SFEF and SDA-1, the bottom phase contains abundant asphaltene, which owns the strong association effect with metals, and thus, the distribution factors of Ni and V are low down to 0.006−0.06 and 0.05−0.10, respectively, (ii) while in SDA-2, the bottom phase contains rare asphaltene (<5%), the association effect of resin is weaker than that of asphaltene, and thus, the distribution factor rises up to 0.3−0.5. It implies that asphaltene could associate abundant metals to pull down the distribution factor. Therefore, it suggests a novel approach for enhancing the efficiency of demetalization by the association effect of asphaltene in SDA processes.

Equations 11 and 13 show that distribution factors of metals are related to the solvent density, association enthalpy, and temperature. On the basis of the assumption of constant b (see the Appendix), the parameters n, b, and ΔH are easily regressed by using SFEF or SDA data. The regressed results are listed in Table 4.

Figure 4 depicts the change of the distribution factor of metal depending upon the solvent density ρ_S, association enthalpy ΔH, and temperature T. Equations 11 and 13 provide the thermodynamics and theoretical guide for removing the metals from the heavy oil. For example, if the solvent density becomes low, the distribution factor of metal in oil will become low; thus, the efficiency of demetalization of SDA will become high. It is coincident with the actual facts.

Although Table 2 lists that the V content of AR or VR is about 4.0−4.5 times higher than the Ni content, their distribution factors and model parameters are near. Therefore, a tuned model could be proposed to describe the distribution factors of both Ni and V between the extraction phase and bottom phase during pentane solvent deasphalting. Figure 5 depicts that the tuned model (n = 4.82, ΔH = −19.1 kJ/mol, and b = 6.282) has been successful in predicting the pilot plant data, and the RSD is 2.6%.

4.4. Physical Significance of the Solvent Association Number. The solvent association number n represents the average number of solvent association. It is a characteristic constant for the given solvents and metal species. Therefore, it may be changed with solvent species and metal species. This work shows that 4.14−5.87 solvent molecules are associated with one DAO molecule in the extract phase during the pentane SDA process. For comparison, the mole ratio of solvent/oil is 50−70:1. It is helpful to imagine the solvent state around the oil molecule in the SDA process.

DOI: 10.1021/ef502696p
Energy Fuels 2015, 29, 1534−1542

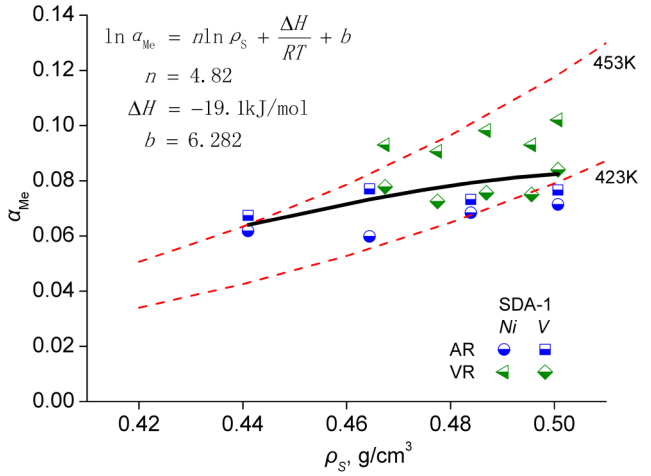

Figure 5. Comparison of Ni and V distribution factors between the predication of the tuned model and experiment data of pentane solvent deasphalting.

4.5. Physical Significance of the Metal Association Enthalpy. For simplification, here, we only discuss the average value of association enthalpy. $\Delta H_2 = \Delta H_S - \Delta H_R = -48.4$ kJ/mol; $\Delta H_1 = \Delta H_S - \Delta H_A = -19.1$ kJ/mol. The inequation $\Delta H_2 < \Delta H_1$ indicates that the apparent solvation of metal in SDA-2 is stronger than that in SDA-1. It indicates that the metal is more easily transferred from the bottom phase to extract phase. Correspondingly, the distribution factor of metal in SDA-2 is higher than that in SDA-1 (Figure 4).

$$\Delta H_2 - \Delta H_1 = (\Delta H_S - \Delta H_R) - (\Delta H_S - \Delta H_A)$$
$$= \Delta H_A - \Delta H_R = -29.3\text{ kJ/mol} \quad (15)$$

The inequation $\Delta H_A < \Delta H_R$ indicates that the association energy of metal−asphaltene is stronger than that of metal−resin because the association is exothermic, which provides a thermodynamic guarantee for enhancing the efficiency of demetalization by the association effect of asphaltene in the SDA process. Correspondingly, the distribution factor of metal in SDA-1 is lower than that in SDA-2 (Figure 4). The result is also helpful to understand why higher Ni and V contents in petroleum are generally coupled by a higher asphaltene content.

The above enthalpy values characterize the association energy change of metals with asphaltene, resin, oil, and solvent. Moreover, these values are in a reasonable range, because the ΔG and ΔH values of the adsorption process between vanadyl porphyrins and asphaltene in room temperature were about −20 and −40 kJ/mol, respectively.[15]

5. CONCLUSION

In this paper, three association models are proposed to describe the metal association equilibrium and combined to determine the metal distribution during the pentane solvent deasphalting process. Three major results are as follows: (1) The model reveals that the distribution factor of Ni or V is related to the solvent density, association enthalpy, and temperature. The model provides the thermodynamics and theoretical guide for removing the metals from the heavy oil. The average difference of enthalpy between solvation enthalpy of metal−DAO−solvent and association enthalpy of metal−asphaltene is −19.1 kJ/mol, and the difference is −48.4 kJ/mol for metal−resin. The association enthalpy of metal−asphaltene is −29.3 kJ/mol, less than that of metal−resin. It indicates that the efficiency of demetalization could be enhanced by the association of asphaltene in the deasphalting process. (2) The distribution factor for Ni and V is generally in the range of 0.006−0.10 when asphaltene exists; however, the distribution factor without asphaltene rises up to about 0.3−0.5. It validated the strong association effect existing between metalloporphyrins and asphaltene.[15] (3) The distribution factors of Ni and V are near, although the V content is much higher than the Ni content. The tuned equation could well-predict the distribution factors for both Ni and V during pentane solvent deasphalting.

Our model provide a new understanding about the association between metal and asphaltene, and it is well-validated by pentane solvent deasphalting; however, the model needs to be improved in the generalization of parameters for other solvent species, more metal species, and more heavy oils under different operation conditions.

APPENDIX

A1. Hypothesis of the Metal Association Model

In this work, the Chrastil model[16] is extended to the ternary system of metal species (Me), DAO (O), and solvent molecule (S). In the extract phase

$$m\text{Me} + p\text{O} + n\text{S} \rightleftarrows \text{Me}_m\cdot\text{O}_p\cdot\text{S}_n \quad (A1)$$

where m, p, and n are the molecule numbers of metal, DAO, and solvent, respectively.

Here, we assume the stoichiometric number: $m/p/n = 1{:}1{:}n$.

Above all, one metalloporphyrin is composed of one metal and one porphyrin mostly according to 1:1.[8−14]

Second, the probability is very low that two or more molecules of Ni and V metals are all congregated into one molecule of oil, because the Ni and V contents are very low (ppm level; see Tables 2 and 3). Thus, $m = 1$ is reasonable.

Third, the probability is very low that two or more molecules of oil are all congregated into one molecule. Because of that, (i) there is no small-molecule oil as a ligand, because small-molecule oils have been distillated away; (ii) the boiling point of petroporphyrins is 565 °C+, and the carbon number is from 25 to 39 and even to 60 (correspondingly, the boiling point of cuts from SFEF or the DAO from SDA is 525°C+, and the carbon number is 30−60); and (iii) in each cut from SFEF, the oil molecules have an approximate molecular weight. With this information combined, one molecule of oil could only contain one petroporphyrin structure. Then, according to metal/porphyrin = 1:1, the probability is very low that two or more big-molecule heavy oils are all congregated with one molecule of metal. Thus, $m/p = 1{:}1$ is reasonable. It is noted that this assumption is also applied in the association model of metal−asphaltene and metal−resin.

Finally, n molecules of solvent are assumed for the solvation effect in the SDA process.

Although some assumptions are based on the theoretical analysis, the regressed results and predicted values show that the assumptions are reasonable (see Tables 2−4 and Figures 4 and 5).

The possible association model of metals in the extract phase is as follows:

$$\text{Me} + \text{O} + n\text{S} \rightleftarrows \text{Me}\cdot\text{O}\cdot\text{S}_n \quad (1)$$

The solution equilibrium constant K_S can be expressed as follows in eq 2

DOI: 10.1021/ef502696p
Energy Fuels 2015, 29, 1534−1542

$$K_S = \frac{[Me{\cdot}O{\cdot}S_n]}{[Me][O][S]^n} \quad (2)$$

$$[O] = c_{O,E}/M_{O,E} \quad (A2)$$

$$[S] = \rho_S/M_S \quad (A3)$$

$$\begin{aligned} c_{Me,E} &= [Me{\cdot}O{\cdot}S_n]M_{Me} \\ &= K_S[Me][O][S]^n M_{Me} \\ &= K_S c_{O,E} M_{O,E}^{-1} \rho_S^n M_S^{-n} [Me] M_{Me} \end{aligned} \quad (A4)$$

where $c_{Me,E}$ is the metal content in the extract phase, $c_{O,E}$ is the oil content in the extract phase, $M_{O,E}$ is the molecular weight of extracted oil, ρ_S is the solvent density, M_S is the molecular weight of solvent, and M_{Me} is the molecular weight of metal.

A2. Distribution Factor of Metal between the Rich-Solvent and Rich-Asphaltene Phases

In the bottom phase of SDA-1 and SFEF, the association of metals mainly depends upon the interaction between metal species and asphaltene

$$Me + Asp \rightleftarrows Me{\cdot}Asp \quad (4)$$

$$K_A = \frac{[Me{\cdot}Asp]}{[Me][Asp]} \quad (5)$$

$$[Asp] = c_{Asp,B}/M_{Asp,B} \quad (A5)$$

$$\begin{aligned} c_{Me,B} &= [Me{\cdot}Asp]M_{Me} + [Me]M_{Me} \\ &\approx [Me{\cdot}Asp]M_{Me} \\ &= K_A[Asp][Me]M_{Me} \\ &= K_A c_{Asp,B} M_{Asp,B}^{-1} [Me] M_{Me} \end{aligned} \quad (A6)$$

where $c_{Me,B}$ is the metal content in the bottom phase, $c_{Asp,B}$ is the asphaltene content in the bottom residue, and $M_{Asp,B}$ is the molecular weight of asphaltene in the bottom phase of SDA-1 or SFEF.

Because the Ni and V contents are very low (ppm level; see Tables 2 and 3), then the metals belong to the less soluble components. In fact, metals are mostly present in the association forms. It implies that the dissociative metal species are much less than the associated metal species. Then, $[Me] \ll [Me{\cdot}Asp]$; therefore, $[Me{\cdot}Asp] + [Me] \approx [Me{\cdot}Asp]$.

From eqs 10, A4, and A6, we can obtain the following equations for the distribution factor of metal:

$$\alpha_{Me} = \frac{K_S c_{O,E} M_{O,E}^{-1} \rho_S^n M_S^{-n}/c_{O,E}}{K_A c_{Asp,B} M_{Asp,B}^{-1}/c_{O,B}} \quad (A7)$$

$$\alpha_{Me} = \frac{K_S}{K_A} \rho_S^n \frac{M_{Asp,B}/M_{O,E}}{M_S^n (c_{Asp,B}/c_{O,B})} \quad (A8)$$

Using logarithmization

$$\ln \alpha_{Me} = \ln K_S - \ln K_A + n \ln \rho_S + \ln \frac{M_{Asp,B}/M_{O,E}}{M_S^n (c_{Asp,B}/c_{O,B})} \quad (A9)$$

From eqs 3 and 6

$$\ln \alpha_{Me} = \left(\frac{\Delta H_S}{RT} + q_S\right) - \left(\frac{\Delta H_A}{RT} + q_A\right) + n \ln \rho_S + \ln \frac{M_{Asp,B}/M_{O,E}}{M_S^n (c_{Asp,B}/c_{O,B})} \quad (A10)$$

$$\ln \alpha_{Me} = n \ln \rho_S + \frac{\Delta H_1}{RT} + b_1 \quad (11)$$

$$\Delta H_1 = \Delta H_S - \Delta H_A \quad (12)$$

$$\begin{aligned} b_1 = {} & q_S - q_A - n \ln M_S + \ln(M_{Asp,B}/M_{O,E}) \\ & - \ln(c_{Asp,B}/c_{O,B}) \end{aligned} \quad (A11)$$

where n is the solvent association number, ρ_S is the solvent density in g/cm^3, and ΔH_1 is the difference between the solvation enthalpy of metal−DAO−solvent and the association enthalpy of metal−asphaltene.

A3. Distribution Factor of Metal between the Rich-Solvent and Rich-Resin Phases

In the bottom phase of SDA-2, the association of metals mainly depends upon the interaction between metal species and resin

$$Me + Re \rightleftarrows Me{\cdot}Re \quad (7)$$

$$K_R = \frac{[Me{\cdot}Re]}{[Me][Re]} \quad (8)$$

$$[Re] = c_{Re,B}/M_{Re,B} \quad (A12)$$

$$\begin{aligned} c_{Me,B} &= [Me{\cdot}Re]M_{Me} + [Me]M_{Me} \\ &\approx [Me{\cdot}Re]M_{Me} \\ &= K_A[Me][Re]M_{Me} \\ &= K_A c_{Re,B} M_{Re,B}^{-1} [Me] M_{Me} \end{aligned} \quad (A13)$$

where $c_{Re,B}$ is the resin content in the bottom phase and $M_{Re,B}$ is the molecular weight of asphaltene in the bottom phase of SDA-2. Similarly, $[Me{\cdot}Re] + [Me] \approx [Me{\cdot}Re]$.

From eqs 10, A4, and A13, we can obtain the following equations for the distribution factor of metal:

$$\alpha_{Me} = \frac{K_S \rho_S^n M_{O,E}^{-1} M_S^{-n}}{K_R c_{Re,B} M_{Re,B}^{-1}/c_{O,B}} \quad (A14)$$

$$\alpha_{Me} = \frac{K_S}{K_R} \rho_S^n \frac{M_{Re,B}/M_{O,E}}{M_S^n (c_{Re,B}/c_{O,B})} \quad (A15)$$

$$\ln \alpha_{Me} = \ln K_S - \ln K_R + n \ln \rho_S + \ln \frac{M_{Re,B}/M_{O,E}}{M_S^n (c_{Re,B}/c_{O,B})} \quad (A16)$$

From eqs 3 and 9

$$\begin{aligned} \ln \alpha_{Me} = {} & \left(\frac{\Delta H_S}{RT} + q_S\right) - \left(\frac{\Delta H_R}{RT} + q_R\right) + n \ln \rho_S \\ & + \ln \frac{M_{Re,B}/M_{O,E}}{M_S^n (c_{Re,B}/c_{O,B})} \end{aligned} \quad (A17)$$

$$\ln \alpha_{Me} = n \ln \rho_S + \frac{\Delta H_2}{RT} + b_2 \quad (13)$$

$$\Delta H_2 = \Delta H_S - \Delta H_R \quad (14)$$

DOI: 10.1021/ef502696p
Energy Fuels 2015, 29, 1534−1542

$$b_2 = q_S - q_R - n \ln M_S + \ln(M_{Re,B}/M_{O,E}) - \ln(c_{Re,B}/c_{O,B}) \quad (A18)$$

where n is the solvent association number, ρ_S is the solvent density in g/cm^3, and ΔH_2 is the difference between the solvation enthalpy of metal−DAO−solvent and the association enthalpy of metal−resin.

A4. Assumption of Constant *b*

Although parameter b of eqs 11 and 13 depends upon seven parameters, b displays a small change in the whole manipulation range. For example, eq A11 shows that parameter b_1 depends upon q_S, q_A, M_S, $M_{Asp,B}$, $M_{O,E}$, $c_{Asp,B}$, and $c_{O,B}$; however, (i)q_S, q_A, and M_S are constants, (ii) both $M_{Asp,B}$ and $M_{O,E}$ increase with the growth of the DAO yield (thus, the ratio of $M_{Asp,B}/M_{O,E}$ displays a small change), and (iii) the ratio of $c_{Asp,B}/c_{O,B}$ is equal to the mole fraction of asphaltene in the bottom phase, which also displays a small change (see Figure 2). For simplification of the regression of eqs 11 and 13, parameter b is assumed as a constant.

Furthermore, the quantitative analyses imply that both b_1 and b_2 are near the constants. Because the enthalpy of eqs 11 and 13 is determined by the interaction between solvent, asphaltene, resin, and metals, for a given SDA system under the given operational conditions, the enthalpy (ΔH_S, ΔH_A, and ΔH_R) and temperature are changeless. Figure A1 shows that ln α_{Me} is almost

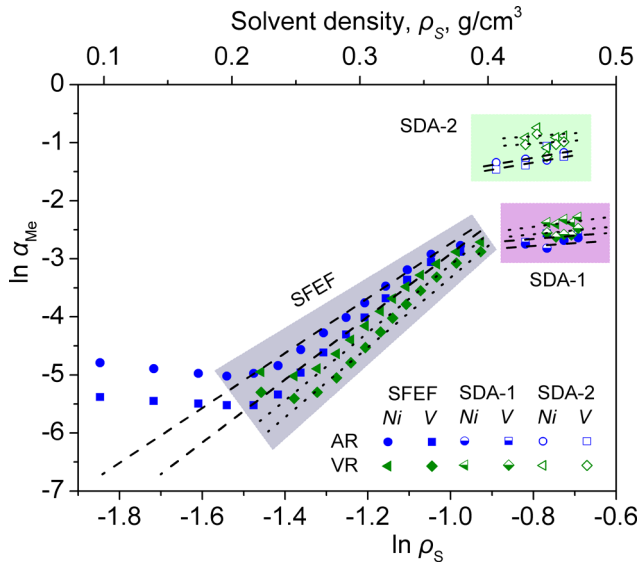

Figure A1. Ni and V distribution factors during pentane solvent deasphalting in ln−ln plot form in SFEF (gray area), SDA-1 (purple area), and SDA-2 (green area).

linear with ln ρ_S. It derives that the parameters of b_1 and b_2 are approximately constant. Although the linear trends display the slight deviations under the low solvent density (<0.2 g/cm^3), for the corresponding 1−4 cuts (Figure 3, <20% yield), the experimental values of Ni and V contents are both less than 10 ppm. Therefore, the assumption of constant b does not pull down the precision of the model. It indicated that the assumption of constant b is reasonable and acceptable. Apparently, constant b is convenient for simplifying the parameter regression of eqs 11 and 13.

AUTHOR INFORMATION

Corresponding Author

*Telephone: +86-10-89739015. Fax: +86-10-69724721. E-mail: sqzhao@cup.edu.cn.

Notes

The authors declare no competing financial interest.

ACKNOWLEDGMENTS

This work was supported by the National "Twelfth Five-Year" Plan for Science and Technology Support (2012BAE05B06), the Union Fund of the National Natural Science Foundation of China (NSFC) and the China National Petroleum Corporation (CNPC) (U1162204), and the NSFC Fund (21176254 and 21376262).

NOMENCLATURE

Abbreviations and Symbols

SFEF = supercritical fluid extraction and fractionation process
SDA = solvent deasphalting process
SELEX-Asp = selective extraction and deasphalting process
SDA-1 and SDA-2 = first and second stages of SELEX-Asp, respectively
RSD = relative standard deviation
Me, O, S, Asp, and Re = metal, oil, solvent, asphaltene, and resin, respectively
K = equilibrium constant
M = molecular weight
c = content or concentration
n = solvent association number
b and q = constants
ρ_S = solvent density
α_{Me} = distribution factor of metal (Ni or V)
ΔH_S = solvation enthalpy of metal−DAO−solvent
ΔH_A = association enthalpy of metal−asphaltene
ΔH_R = association enthalpy of metal−resin

Subscripts

Me, O, S, Asp, and Re = metal, oil, solvent, asphaltene, and resin, respectively
E and B = extract and bottom phases in the SDA process, respectively

REFERENCES

(1) Rana, M. S.; Sámano, V.; Ancheyta, J.; Diaz, J. A. I. A review of recent advances on process technologies for upgrading of heavy oils and residue. *Fuel* **2007**, *86* (9), 1216−1231.
(2) Furimsky, E. Lowered emissions schemes for upgrading ultra heavy petroleum feeds. *Ind. Eng. Chem. Res.* **2009**, *48* (6), 2752−2769.
(3) Speight, J. G. Deasphalting and dewaxing processes. In *The Refinery of the Future*; William Andrew Publishing: Boston, MA, 2011; Chapter 7, pp 209−236.
(4) Cao, F.; Jiang, D.; Li, W.; Du, P.; Yang, G.; Ying, W. Process analysis of the extract unit of vacuum residue through mixed C4 solvent for deasphalting. *Chem. Eng. Process.* **2010**, *49* (1), 91−96.
(5) Shui, H.; Shen, B.; Gao, J. Investigation of vacuum residue solubility in a C4 solvent. *Fuel* **1998**, *77* (8), 885−889.
(6) Ali, M. F.; Abbas, S. A review of methods for the demetallization of residual fuel oils. *Fuel Process. Technol.* **2006**, *87* (7), 573−584.
(7) Miller, J. T.; Fisher, R. B.; van der Eerden, A. M. J.; Koningsberger, D. C. Structural determination by XAFS spectroscopy of non-porphyrin nickel and vanadium in Maya residuum, hydrocracked residuum, and toluene-insoluble solid. *Energy Fuels* **1999**, *13* (3), 719−727.
(8) Rodgers, R. P.; Hendrickson, C. L.; Emmett, M. R.; Marshall, A. G.; Greaney, M.; Qian, K. N. Molecular characterization of petroporphyrins in crude oil by electrospray ionization Fourier transform ion cyclotron resonance mass spectrometry. *Can. J. Chem.* **2001**, *79* (5−6), 546−551.

DOI: 10.1021/ef502696p
Energy Fuels 2015, 29, 1534−1542

(9) McKenna, A. M.; Purcell, J. M.; Rodgers, R. P.; Marshall, A. G. Identification of vanadyl porphyrins in a heavy crude oil and raw asphaltene by atmospheric pressure photoionization Fourier transform ion cyclotron resonance (FT-ICR) mass spectrometry. *Energy Fuels* **2009**, *23* (4), 2122−2128.
(10) Qian, K.; Mennito, A. S.; Edwards, K. E.; Ferrughelli, D. T. Observation of vanadyl porphyrins and sulfur-containing vanadyl porphyrins in a petroleum asphaltene by atmospheric pressure photonionization Fourier transform ion cyclotron resonance mass spectrometry. *Rapid Commun. Mass Spectrom.* **2008**, *22* (14), 2153−2160.
(11) Qian, K.; Edwards, K. E.; Mennito, A. S.; Walters, C. C.; Kushnerick, J. D. Enrichment, resolution, and identification of nickel porphyrins in petroleum asphaltene by cyclograph separation and atmospheric pressure photoionization Fourier transform ion cyclotron resonance mass spectrometry. *Anal. Chem.* **2009**, *82* (1), 413−419.
(12) Zhao, X.; Liu, Y.; Xu, C.; Yan, Y.; Zhang, Y.; Zhang, Q.; Zhao, S.; Chung, K.; Gray, M. R.; Shi, Q. Separation and characterization of vanadyl porphyrins in Venezuela Orinoco heavy crude oil. *Energy Fuels* **2013**, *27* (6), 2874−2882.
(13) Shiraishi, Y.; Hirai, T.; Komasawa, I. A novel demetalation process for vanadyl- and nickelporphyrins from petroleum residue by photochemical reaction and liquid−liquid extraction. *Ind. Eng. Chem. Res.* **2000**, *39* (5), 1345−1355.
(14) Yin, C. x.; Stryker, J. M.; Gray, M. R. Separation of petroporphyrins from asphaltenes by chemical modification and selective affinity chromatography. *Energy Fuels* **2009**, *23* (5), 2600−2605.
(15) Chen, F.; Liu, Q.; Xu, Z.; Sun, X.; Shi, Q.; Zhao, S. Adsorption kinetics and thermodynamics of vanadyl etioporphyrin on asphaltene in pentane. *Energy Fuels* **2013**, *27* (11), 6408−6418.
(16) Chrastil, J. Solubility of solids and liquids in supercritical gases. *J. Phys. Chem.* **1982**, *86* (15), 3016−3021.
(17) Škerget, M.; Knez, Z.; Knez-Hrnčič, M. Solubility of solids in sub- and supercritical fluids: A review. *J. Chem. Eng. Data* **2011**, *56* (4), 694−719.
(18) Zhao, S.; Wang, R.; Lin, S. High-pressure phase behavior and equilibria for chinese petroleum residua and light hydrocarbon systems. Part II. *Pet. Sci. Technol.* **2006**, *24* (3/4), 297−318.
(19) Eslamimanesh, A.; Mohammadi, A. H.; Richon, D. Determination of sulfur content of various gases using Chrastil-type equations. *Ind. Eng. Chem. Res.* **2011**, *50* (12), 7682−7687.
(20) Eslamimanesh, A.; Mohammadi, A. H.; Yazdizadeh, M.; Richon, D. Chrastil-type approach for representation of glycol loss in gaseous system. *Ind. Eng. Chem. Res.* **2011**, *50* (17), 10373−10379.
(21) G-Hourcade, M. L.; Torrente, C.; Ángel Galán, M. Study of the solubility of kerogen from oil shales (Puertollano, Spain) in supercritical toluene and methanol. *Fuel* **2007**, *86* (5−6), 698−705.
(22) Torrente, M. C.; Galán, M. A. Extraction of kerogen from oil shale (Puertollano, Spain) with supercritical toluene and methanol mixtures. *Ind. Eng. Chem. Res.* **2010**, *50* (3), 1730−1738.
(23) Gutiérrez, C.; Rodríguez, J. F.; Gracia, I.; de Lucas, A.; García, M. T. Modeling the phase behavior of essential oils in supercritical CO_2 for the design of a countercurrent separation column. *Ind. Eng. Chem. Res.* **2014**, *53* (32), 12830−12838.
(24) Shi, T. P.; Hu, Y. X.; Xu, Z. M.; Su, T.; Wang, R. A. Characterization index of petroleum vacuum resudua. *Acta Pet. Sin., Pet. Process. Sect.* **1997**, No. 2, 5−11.
(25) Yang, G.; Wang, R. The supercritical fluid extractive fractionation and the characterization of heavy oils and petroleum residue. *J. Pet. Sci. Eng.* **1999**, *22*, 47−52.
(26) Zhao, S.; Xu, C.; Sun, X.; Chung, K. H.; Xiang, Y. China refinery tests asphaltenes extraction process. *Fuel Process. Technol.* **2010**, *108* (12), 52.
(27) Zhao, S.; Xu, Z.; Xu, C.; Chung, K. H.; Wang, R. Systematic characterization of petroleum residua based on SFEF. *Fuel* **2005**, *84* (6), 635−645.
(28) Zhao, S.; Xu, Z.; Xu, C.; Chung, K. H. Feedstock characteristic index and critical properties of heavy crudes and petroleum residua. *J. Pet. Sci. Eng.* **2004**, *41* (1−3), 233−242.
(29) Xu, Z.; van den Berg, F. G. A.; Sun, X.; Xu, C.; Zhao, S. Detailed characterization of virgin heavy oil resid and its thermally cracked resid. *Energy Fuels* **2014**, *28* (3), 1664−1673.
(30) Zhao, S.; Xu, C.; Sun, X. W.; Chung, K. H.; Xiang, Y. China refinery tests asphaltenes extraction process. *Oil Gas J.* **2010**, *108* (12), 52−58.

DOI: 10.1021/ef502696p
Energy Fuels 2015, 29, 1534−1542